Resonant valence-band and Cu 3p photoemission at the Cu L_3 threshold of $Bi_2Sr_2CuO_6$ and $Bi_2Sr_2CaCu_2O_8$

M. Qvarford, J. F. van Acker, J. N. Andersen, R. Nyholm, I. Lindau, G. Chiaia, and E. Lundgren
Department of Synchrotron Radiation Research, Institute of Physics, Lund University, Sölvegatan 14, S-223 62 Lund, Sweden and MAX-lab, Lund University, Box 118, S-221 00 Lund, Sweden

S. Söderholm, U. O. Karlsson, and S. A. Flodström
Materials Physics, Department of Physics, Royal Institute of Technology, S-100 44 Stockholm, Sweden

L. Leonyuk
Moscow State University, Department of Geology, 119 899 Moscow, Russia
(Received 7 July 1994)

Utilizing monochromatized synchrotron radiation strong photoemission enhancements in the valence-band region and the Cu 3p core level have been measured in the vicinity of the Cu L_3 threshold of $Bi_2Sr_2CuO_6$ and $Bi_2Sr_2CaCu_2O_8$ superconductors. For both the valence-band and the Cu 3p level in both crystals the satellite structures show the strongest enhancements. The line shapes of these enhanced satellites are shown to be in good agreement with calculated atomic Auger spectra for the $3d^8$ and $3p^5 3d^9$ final states, respectively. Measurements of the valence-band emission in $Bi_2Sr_2CaCu_2O_8$ using a number of different photon energies in the vicinity of the Cu L_3 threshold show that the enhancement occurs at a constant binding energy for photon energies tuned to the low-energy flank of the Cu L_3 x-ray-absorption peak. This behavior supports the interpretation that the enhancement is due to a photoemission resonance. The implications of the copper nature of the valence-band satellite on the description of the electronic structure of these compounds are briefly discussed.

I. INTRODUCTION

Since the discovery of Cu-O-based high-T_c superconductors[1] (HTSC) the importance of correlation effects among the Cu d electrons has been widely discussed and investigated both theoretically and experimentally.[2] It has, for instance, been found that a band-structure calculation[3] for La_2CuO_4, the mother compound of $La_{2-x}Sr_xCuO_4$, predicts a metallic ground state, in contrast to the measured band gap of about 2 eV.[4] Also, comparison of measured valence-band photoemission spectra and those calculated from band theory for La_2CuO_4 and $La_{2-x}Sr_xCuO_4$ gives poor agreement.[5,6] For $Bi_2Sr_2CaCu_2O_8$ valence-band photoemission spectra calculated from a band theory approach[7] give for photon energies around 100 eV a maximum in intensity at around 1 eV binding energy, clearly different from measured valence-band photoemission spectra. Fujimori *et al.*[6] find that the agreement between theoretical and experimental valence-band spectra is clearly improved with a theoretical spectrum obtained from a configuration-interaction cluster calculation which, in contrast to the band-structure calculations, explicitly takes into account the intra-atomic Coulomb interaction, U_{dd}, between d electrons.

The cluster calculation by Fujimori *et al.*[6] also predicts a valence-band satellite at around 11–12 eV binding energy assigned to the Cu $3d^8$ final state which is pushed away from the main valence band due to the large U_{dd}. In order to judge whether electron correlation among the Cu 3d electrons is essential for the description of the electronic structure it is important to identify if such a valence-band satellite exists. This can be done by resonant photoemission for photon energies tuned to a Cu p level, for instance the $M_{2,3}$ or L_3 thresholds. The Cu $M_{2,3}$ threshold is easier to access experimentally and resonant photoemission at the Cu $M_{2,3}$ threshold is a standard tool to probe such a satellite in the valence bands of Cu-O compounds. In CuO,[8] $YBa_2Cu_3O_7$,[9–11] and $La_{2-x}Sr_xCuO_4$,[10] an enhancement of the emission at a binding energy of 12–13 eV has been found for photon energies tuned to the Cu $M_{2,3}$ threshold, measurements which show the satellite's copper nature. However, the same type of measurements have given rise to a comparatively weaker resonant enhancement at the expected satellite position in $Bi_2Sr_2CaCu_2O_8$ and $Bi_2Sr_2CuO_6$.[2,12]

It has recently been demonstrated, both theoretically and experimentally, that photoemission resonance phenomena orders of magnitudes larger than at the shallower $M_{2,3}$ thresholds can be observed at the L_3 threshold in Ni (Refs. 13–15) and Cu-O compounds.[16–18] In this way weak satellite structures can be studied and such measurements have, for instance, provided an unambiguous identification of the Cu $3d^8$ valence-band final state in CuO, showing the charge-transfer nature of the insulating gap.[16]

The measurements presented in this report were performed both on $Bi_2Sr_2CuO_6$ (low-T_c) as well as on $Bi_2Sr_2CaCu_2O_8$ (high-T_c) single crystals in order to compare two superconductors with rather similar crystal

structure and stoichiometry, but different T_c. The spectra show strong photoemission enhancements in the valence band for photon energies tuned to the Cu L_3 threshold of the two Cu-O based superconductors. The strongest valence-band enhancement is found at a binding energy of about 12.5 eV, unambiguously demonstrating the existence of a copper derived valence-band satellite in both compounds. Similarly, strong enhancements and satellite structures are also seen in the Cu 3p core level for photon energies tuned to the Cu L_3 threshold. The latter effect for Cu-O compounds has previously only been predicted theoretically,[17] but is demonstrated experimentally in the present work. To our knowledge, resonant photoemission measurements at the Cu L_3 edge of Cu-O based superconductors have only been reported[18] for the valence-band region in $Bi_2Sr_2CaCu_2O_8$, showing an enhancement similar to the one found in the present work.

II. EXPERIMENTAL

The measurements were performed at beamline 22 at the MAX national synchrotron-radiation laboratory in Lund, Sweden. The beamline is equipped with a modified Zeiss SX-700 plane grating monochromator.[19,20] X-ray-absorption (XAS) spectra were recorded by detecting the total electron yield using a channeltron. A Scienta-type hemispherical electron energy analyzer (200-mm mean radius) with a multichannel detector system[20] was used to record the photoemission spectra. For the photoemission spectra at the Cu L_3 edge, the photon energy resolution and electron energy resolution were about 1.4 and 0.6 eV, respectively (the XAS spectra displayed in Fig. 1 were measured at a higher photon energy resolution, ~0.8 eV). Valence-band spectra were also measured at a photon energy of 100 eV with a total-energy resolution of about 0.1 eV. The photoemission binding-energy scale was determined with reference to the Fermi edge. At photon energies around the Cu L_3 edge the binding-energy calibration was done by aligning the Bi 5d core level to the calibrated binding energy obtained at 100-eV photon energy. The absolute values of the photon energies used around the Cu L_3 edge were calibrated according to the procedure described in Ref. 21.

$Bi_2Sr_2CuO_6$ and $Bi_2Sr_2CaCu_2O_8$ single crystals were glued with conducting silver epoxy to the sample holder. Clean samples were obtained by cleaving *in situ*, at a pressure below 10^{-10} Torr. The growth method of the $Bi_2Sr_2CaCu_2O_8$ crystals is described elsewhere.[22] The $Bi_2Sr_2CaCu_2O_8$ structure has a subunit cell containing two CuO_2 planes separated by a Ca layer[23–25] and T_c of samples similar to the one used in the present study has been determined to be 90 K.[22] The $Bi_2Sr_2CuO_6$ crystal was grown from a stoichiometric melt, $Bi_2O_3+2\ SrCO_3 + CuO$, heated to 1050 °C in an alumina crucible and then cooled down. The heating and cooling rate was 10 °C/h. The microprobe analysis result is consistent with the ideal stoichiometry (2:2:0:1): $Bi_{2.26}Sr_{1.74}Cu_{0.99}O_{6+\delta}$. X-ray-diffraction measurement shows that the crystal is of a single phase with lattice parameters $a=3.8$ Å and $c=24.6$ Å. $Bi_2Sr_2CuO_6$ has a crystal structure which is quite similar to the structure of $Bi_2Sr_2CaCu_2O_8$, but contains no Ca and has only one CuO_2 plane in the subunit cell.[24–26] T_c of the $Bi_2Sr_2CuO_6$ sample was determined, by means of magnetic measurements, to be around 20 K.

III. RESULTS AND DISCUSSION

Figure 1 shows photoemission spectra for $Bi_2Sr_2CaCu_2O_8$ (Bi2212, left panel) and $Bi_2Sr_2CuO_6$ (Bi2201, right panel) measured at three different photon energies in the vicinity of the Cu L_3 edge. The spectra are normalized to equal Bi 5d intensity, which corresponds to a normalization to the photon flux since the Bi 5d photoionization cross section is almost constant in this photon energy interval.[27] In spectra *B*, measured at the maximum of the Cu L_3 edge, both samples show very strong enhancements in the valence-band and Cu 3p re-

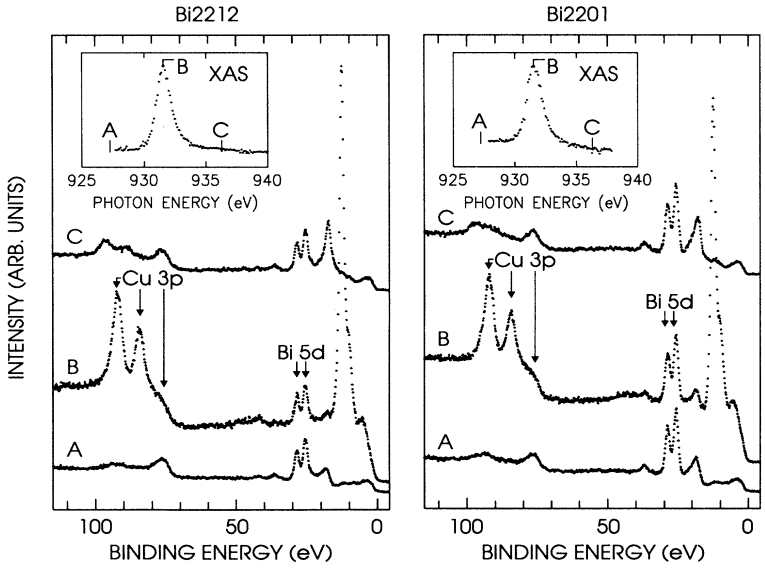

FIG. 1. Valence band through Cu 3p photoemission spectra for $Bi_2Sr_2CaCu_2O_8$ (left panel) and $Bi_2Sr_2CuO_6$ (right panel) measured with three different photon energies in the vicinity of the Cu L_3 absorption edge. The corresponding XAS spectra are shown in the insets in which the photon energies used for spectra *A*-*C* are marked.

gions. Comparing the on-resonance spectra (B) with the off-resonance spectra (A and C) it is clear that for both the valence-band and the Cu $3p$ regions it is the satellite structures which show the stronger enhancement at resonance for both crystals. The weak structures seen in the binding energy (BE) regions of the satellite structures in the off-resonance spectra (A) could also be due to the Bi $6s$ ($\sim$12 eV) and Bi $5p_{3/2}$ ($\sim$93 eV) emissions. In the BE region immediately below the Bi $5d$ level are the Ca $3p$, O $2s$, and Sr $4p$ levels, the strongest emission arising from Sr $4p$ ($\sim$18 eV).

In order to more clearly display the strong enhancements which are seen when the photon energy is tuned to the Cu L_3 absorption maximum, Fig. 2 shows the result of subtracting the off-resonance spectrum (A) from the on-resonance spectrum (B) for Bi2212. For this compound the BE scale was expanded in order to also include the Cu $3s$ and Sr $3d$ levels. It is clearly seen in the subtraction spectrum that it is not only the valence-band satellite but also the main valence-band emission at lower BE ($\sim$5 eV) which is enhanced at resonance.[28] As seen in Fig. 2, this enhancement of the main valence band seems to be comparatively stronger than the enhancement of the Cu $3p$ main line ($\sim$76 eV). For Ni, resonant photoemission measurements[15] at the Ni L_3 threshold have resulted in an enhanced satellite structure also in the $3s$ level. For the present compounds the expected BE for a Cu $3s$ satellite is partly overlapped by the strong Sr $3d$ emission ($\sim$132 eV). However, from the subtraction spectrum in Fig. 2, in which the Sr $3d$ signal is depleted, it is concluded that the enhancement of a Cu $3s$ satellite, if it exists, is very weak in Bi2212.

The XAS spectra in Fig. 1 show a single sharp peak quite similar to the Cu L_3 XAS spectrum of CuO. These XAS spectra are clearly different in threshold energy and shape from the Cu L_3 XAS spectra of Cu_2O and Cu metal.[18,29] This indicates a divalent ($3d^9$) nature of Cu in both Bi2212 and Bi2201. From this observation the excitation and deexcitation processes studied in spectra B in Fig. 1 can be written, in terms of the electron configuration of the relevant levels, in the following way for the valence-band (1) and the $3p$ level (2):

$$h\nu + 2p^6 3p^6 3d^9 \rightarrow 2p^5 3p^6 3d^{10} \begin{cases} \rightarrow 2p^6 3p^6 3d^8 + \varepsilon_k & (1) \\ \rightarrow 2p^6 3p^5 3d^9 + \varepsilon_k \, . & (2) \end{cases}$$

The first transition in (1) and (2) is the X-ray-absorption process in which a photon of energy $h\nu$ excites a $2p$ electron to a localized $3d$ orbital yielding a bound $2p^5 3d^{10}$ intermediate state. The second transition is of Auger type giving a singly ionized final state and an emitted electron, ε_k. Since the final states are singly ionized they can also be reached by direct photoemission and a resonance enhancement of the photoemission features can occur.

From the above reasoning the enhanced satellite structures are assigned to the $3d^8$ and $3p^5 3d^9$ final states for the valence band and the $3p$ level, respectively. The dominating off-resonance photoemission, at lower BE than the satellite structures seen on resonance, is attributed to the $3d^9\underline{L}$ ($\underline{L}$=ligand hole) and $3d^{10}\underline{L}^2$ final states for the valence band and the $3p^5 3d^{10}\underline{L}$ final state for the $3p$ core level. The presently found splitting of the Cu $3p$ level into main-line and satellite structures in Bi2212 and Bi2201 is similar to the well-known splitting of the Cu $2p$ level in HTSC compounds.[30] These assignments of the satellite structures in Cu $3p$ and $2p$ core-level spectra of HTSC compounds are the same as those earlier established for copper dihalides by van der Laan *et al.*[31]

The assignments of the resonating satellite structures are confirmed by atomic Auger calculations. The intensities of the Auger lines were calculated in a mixed coupling scheme.[32–34] In this treatment the Auger initial state consists of a single inner shell hole, all other shells being complete. The atomic radial wave functions were calculated by means of the Hartree-Fock method.[35] From these wave functions the radial part of the continuum state, needed to compute radial matrix elements, was calculated in a Hartree-Fock-Slater scheme.[36] The relative energy positions of the multiplet lines were determined by means of a multiconfigurational Dirac-Fock program.[37] In order to obtain acceptable agreement with the experimental results, full configuration interaction should be taken into account. In the present calculations this has been approximated by compressing the energy scale to 85% of its original value, which corresponds to a renormalization of the radial integrals involved by the same factor.

Figure 3(a) displays, from bottom, the calculated atomic Auger multiplets for the Cu $3p^5 3d^9$ final state, the calculated spectrum convoluted with a Lorentzian function of a full width at half maximum (FWHM) of 2.0 eV and a Gaussian function of FWHM 1.5 eV, and the Cu $3p$ region of spectrum B for Bi2212 in Fig. 1. Figure 3 (b) shows a similar set of spectra for the valence-band region, but now the Auger calculation is done for the Cu $3d^8$

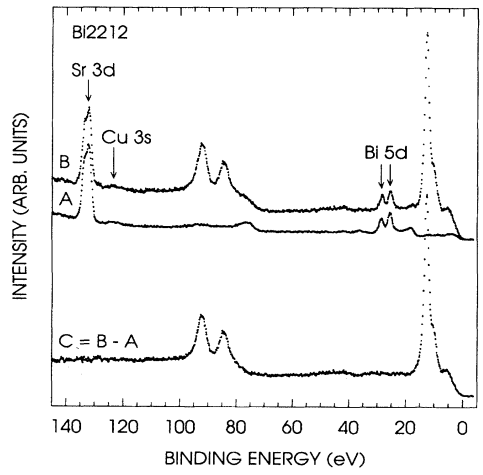

FIG. 2. Valence band through Sr $3d$ photoemisson spectra for $Bi_2Sr_2CaCu_2O_8$ measured below the Cu L_3 absorption threshold (A) and at the Cu L_3 absorption maximum (B). The photon energies used are the same as for spectra A and B in Fig. 1 for $Bi_2Sr_2CaCu_2O_8$. At the bottom is shown the result of subtracting spectrum A from spectrum B.

final state, and the convolution is done with a Lorentzian function of FWHM 0.8 eV and a Gaussian function of FWHM 1.5 eV. The Gaussian width corresponds to the estimated instrumental resolution. The dominating line in the $3d^8$ Auger multiplet is the ^1G line. The different Lorentzian broadenings needed to fit the calculated spectra to the measured ones indicates that the lifetime for the $3p^5 3d^9$ final state is shorter than for the $3d^8$ final state due to the possibility that the $3p^5 3d^9$ final state can decay by a $M_{2,3}VV$ super Coster-Kronig channel.

It is clearly seen in Fig. 3 that the lineshape of the resonating satellites is well reproduced by these atomic Auger calculations.[38] This computational scheme works well at the Cu L_3 threshold in these Cu-O based superconductors for two reasons. Firstly, in the intermediate state, which is the Auger initial state, the $3d$ shell is filled, i.e., Cu is in a $3d^{10}$ state. Secondly, as has been pointed out in previous work,[14,15,17] the cross section of the direct photoemission process at resonance is comparatively so low that the interference effect with the intense indirect process, i.e., via the intermediate state, can be neglected in the calculational scheme. Note that this situation is in contrast to the appearance of the Cu $3d^8$ satellite at the Cu $M_{2,3}$ edge. In the latter case the Fano theory should be included in a theoretical treatment.[8,39]

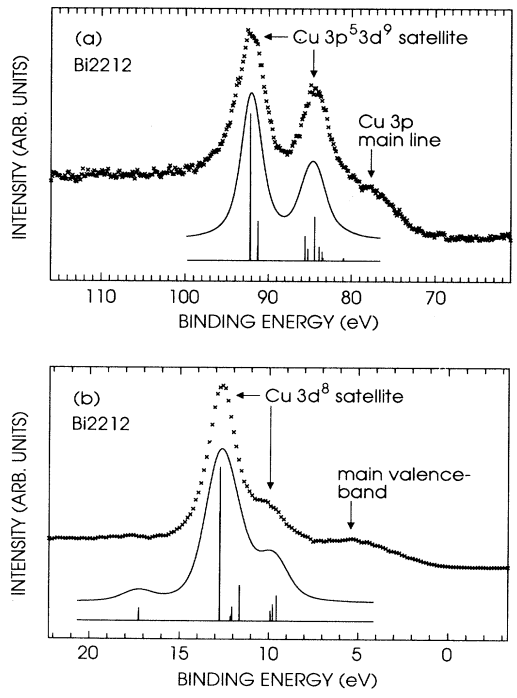

FIG. 3. The upper spectra (crosses) in plot *a* and *b* show, respectively, the Cu 3*p* region and the valence-band region of spectrum *A* for $Bi_2Sr_2CaCu_2O_8$ in Fig. 1. The two lower spectra in each plot display from bottom the calculated atomic Auger multiplet for the $3p^5 3d^9$ (a) and $3d^8$ (b) final states and the same theoretical spectrum but broadened in order to resemble the experimental spectrum. The binding energy of the structure on the low-energy side in the experimental spectra corresponds, respectively, to the position of the Cu 3*p* main line and the main valence band seen in spectra measured off resonance (cf. spectra *A* and *C* in Fig. 1).

In a comprehensive discussion of photoemission enhancements at the excitation threshold of a deeper lying core level it is important to consider whether the enhancement is due to a true photoemission resonance or is simply due to an enhanced Auger emission caused by the large production of core holes at the absorption edge. A requisite for having a resonant photoemission event is that the excited electron in the intermediate state in (1) and (2) stays localized at the copper site. If this is not the case the intensity enhancement at the threshold will arise from a doubly ionized final state and the emitted electron in the final state will have a constant kinetic energy as a function of photon energy through the threshold. Such behavior is in contrast to the constant binding energy which is the case for the singly ionized final states in (1) and (2).

Among the work on resonant photoemission at the L_3 threshold of Ni and Cu-O compounds there is one work[40] which states that the strong intensity enhancement in the valence-band on resonance is simply due to an addition of a strong L_3VV Auger signal to a weak photoemission resonance. In the present work this possibility has been investigated by collecting a number of valence-band photoemission spectra for Bi2212 using different photon energies ranging from ~929 to 935 eV, i.e., across the Cu L_3 absorption peak, with a difference of 0.85 eV between each photon energy. The intensity data from these spectra are displayed as a contour plot in Fig. 4. The contour lines are analogous to the height curves on a topographic map. In order to follow the changes in intensity for the less intense regions in the contour plot without using an extreme amount of contour lines, Fig. 4 shows the logarithm of the measured intensities. The photon energies indicated with arrows are the ones at which the actual measurements were performed.

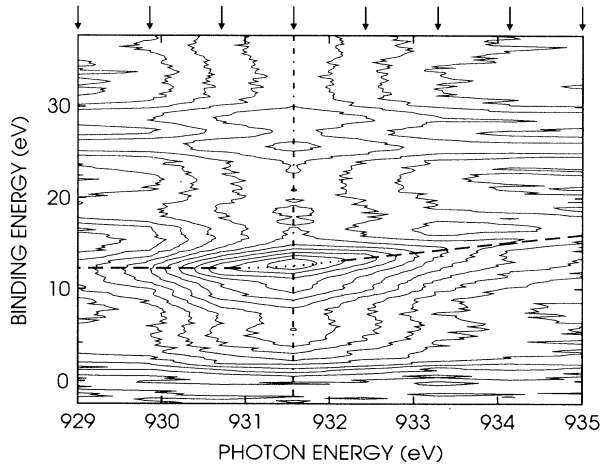

FIG. 4. Contour plot displaying the photoemission intensity in the valence-band region of $Bi_2Sr_2CaCu_2O_8$ as a function of binding energy and photon energy in the vicinity of the Cu L_3 absorption edge. The arrows at top mark the photon energies at which the measurements were performed. Further details are given in the text.

The photon energy dependency of several shallow photoemission features can be seen in Fig. 4. These features are most easily identified by studying Fig. 4 along a constant photon energy line (the dashed-dotted line in Fig. 4) at 931.6 eV, i.e., at the Cu L_3 absorption maximum. From the Fermi level down to about 8-eV BE the enhanced emission from the main valence band is seen followed by the strongly enhanced satellite feature at around 12-eV BE. At around 18-eV BE the plot shows some intensity from the Sr 4*p* level and in the 25–30-eV BE region the Bi 5*d* doublet is clearly seen. These latter shallow core levels seem also to be enhanced at the Cu L_3 threshold energy. This is, however, not true enhancements but is simply due to an increased inelastic background from the enhanced valence-band features.

If we focus our attention on the BE region around 12 eV it is seen in Fig. 4 that for increasing photon energy below the absorption maximum (931.6 eV), the intensity of the 12-eV satellite increases along a constant binding energy, as marked by the dashed line. However, for increasing photon energy above the absorption maximum the enhanced satellite declines and shifts away from the constant binding energy; it follows the dashed line which now is drawn to show the binding-energy shift for a constant kinetic energy feature. It is thus concluded from Fig. 4 that on the low-energy flank of the absorption peak a singly ionized final state is reached according to the description in (1), whereas on the high-energy flank the emission arises from a doubly ionized Auger final state. At the absorption maximum there is a crossover region, marked by the dotted line, showing a small deviation from the constant binding energy. In this context it can be noted that essentially the same photon energy dependence for the satellite binding energy position as shown in Fig. 4 can be seen in the original work on this resonant photoemission process in CuO by Tjeng *et al.*[16] It can also be pointed out that the conclusion about a dominating Auger emission instead of resonant photoemission in CuO by López *et al.*[40] is based on spectra measured using only a few different photon energies in the vicinity of the Cu L_3 edge, none of which was tuned to the low-energy flank of the absorption peak.

Having established that the enhanced valence-band satellite can be assigned to a singly ionized $3d^8$ final state some of its implications concerning the description of the electronic structure in the studied compounds will be briefly discussed. Figure 5 shows the valence-band regions (*C*: Bi2212 and *D*: Bi2201) measured with photon energies tuned to the low-energy flank of the Cu L_3 absorption edge (about 1 eV below the absorption maximum) together with high-resolution valence-band spectra (*A*: Bi2212 and *B*: Bi2201) measured at 100-eV photon energy. The clearest difference between the two samples seen in Fig. 5 is that the maximum of the valence-band emission off resonance is shifted to higher BE in Bi2201 as compared to Bi2212. The dominating $3d^8$ emission on resonance shows only a small shift between the two compounds. The difference between Bi2212 and Bi2201 seen in spectra *A* and *B* agrees well with what has been reported by Shen *et al.*,[12] but is not fully consistent with the results of Lindberg *et al.*[41] The energy

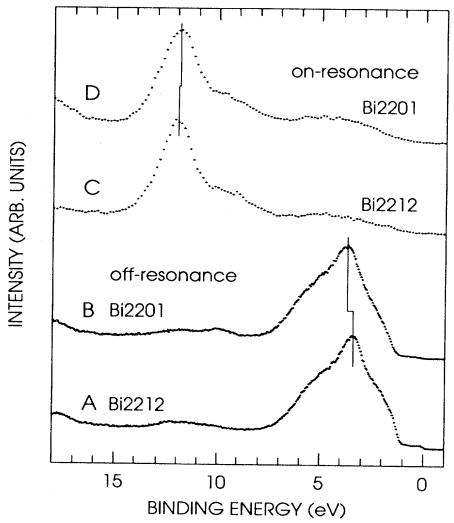

FIG. 5. High-resolution valence-band spectra ($h\nu = 100$ eV) for $Bi_2Sr_2CaCu_2O_8$ (*A*) and $Bi_2Sr_2CuO_6$ (*B*) compared to the corresponding on-resonance photoemission spectra measured at a photon energy about 1 eV below the Cu L_3 absorption maximum (*C* and *D*). The spectra are normalized to equal peak intensity.

difference between the $3d^8$ state and the main valence-band off resonance, ΔE_{VB}, is in the first approximation, neglecting hybridization effects, equal to $U_{dd} - \Delta_{pd}$, Δ_{pd} being the O 2*p* to Cu 3*d* charge-transfer energy.[42] This energy difference is thus slightly different for the two compounds, Bi2212: 8.6 eV, Bi2201: 8.2 eV, with the energy positions defined as marked in Fig. 5, i.e., the position of the $3d^8$ state is mainly determined by the ^1G line.[43] The fact that ΔE_{VB} is large means that the Coulomb repulsion between *d* electrons, U_{dd}, is much larger than Δ_{pd}. This shows that these superconductors belong to the charge-transfer regime in the Zaanen-Sawatzky-Allen (ZSA) phase diagram for transition-metal compounds.[42] From studies of late transition-metal dihalides it has been found that U_{dd} stays nearly constant for each transition-metal cation, whereas Δ_{pd} changes depending on the choice of anion.[44] In analogy it can be expected, provided the effect on ΔE_{VB} from the hybridization shifts is similar for the two samples, that the smaller value for ΔE_{VB} in Bi2201 is caused by Δ_{pd} being larger in Bi2201 than in Bi2212,[45] probably reflecting the different coordination of the oxygen anions near copper in the two compounds.[23–26]

The present measurements also give some additional general information about the electronic structure in Bi2212 and Bi2201. First, the BE of the $3d^8$ state for both Bi2201 and Bi2212 is the same as in CuO within 0.2 eV, but clearly different from the energy position, ~15 eV, of the main intensity enhancement in the valence-band region of Cu_2O at resonance.[8,18] These observations show once again the similarity between Bi2201, Bi2212, and the divalent copper in CuO. In view of the differences in the crystal structure between Bi2201 and Bi2212 (Refs. 23–26) at the copper site, the similar behavior of copper in these compounds in high-energy spectroscopies may be

surprising. In Bi2201 copper is in a sixfold-coordinated, distorted octahedral, site with respect to the oxygen anions, whereas in Bi2212, copper is in a fivefold pyramidal site. The lower oxygen coordination for copper in Bi2212 is caused by the fact that the crystal structure of Bi2212 contains an oxygen deficient, ionic,[46] Ca layer on one side of the CuO_2 planes. The anion-cation relation near copper is thus lower in Bi2212 than in Bi2201 and as a consequence it could be expected that copper would have a lower valence in Bi2212 as compared to Bi2201. However, this effect is compensated for by the fact that the stoichiometric cell of Bi2212 contains two CuO_2 planes separated by the Ca layer. In a simple ionic description the CuO_2-Ca-CuO_2 slab in Bi2212 and the CuO_2 plane in Bi2201 have the same resulting copper valence, divalent, provided one electron is supplied from each of the BiO planes in both compounds. According to this description bismuth is trivalent in both compounds.

Second, the result that Bi2201 and Bi2212 belong to the charge-transfer regime in the ZSA phase diagram means that charge fluctuations of the type $d^9d^9 \rightarrow d^8d^{10}$ are prohibited, because the $3d^8$ state is too high in energy. This implies, as has been pointed out by Fuggle *et al.*,[5] that the $3d^8$ configuration need not be considered in the description of the ground state, i.e., in a cluster-configuration approach the $3d^9$ and $3d^{10}\underline{L}$ states form a complete basis set for the ground state of divalent copper in these compounds.

IV. SUMMARY

In summary, strong enhancements of satellite structures in the Cu 3p and valence-band regions have been measured at the Cu L_3 threshold in $Bi_2Sr_2CaCu_2O_8$ and $Bi_2Sr_2CuO_6$. The assignments of the enhanced satellites to the Cu $3p^5 3d^9$ and Cu $3d^8$ final states are confirmed by atomic Auger calculations. The high binding energy of the Cu $3d^8$ final state as compared to the main valence band shows that the Coulomb interaction U_{dd} is much larger than the charge-transfer energy Δ_{pd} in both compounds. Comparison of the binding energy of the dominating valence-band emission both on and off resonance indicates that the difference between the parameters U_{dd} and Δ_{pd} is slightly larger for $Bi_2Sr_2CaCu_2O_8$ as compared to $Bi_2Sr_2CuO_6$.

ACKNOWLEDGMENTS

We gratefully acknowledge Dr. Z.-X. Shen for providing the $Bi_2Sr_2CaCu_2O_8$ sample and Dr. J. Costa-Krämer and Professor K. V. Rao for performing the magnetization measurement of the $Bi_2Sr_2CuO_6$ sample. This work was supported by the Swedish Natural Science Research Council and the Swedish Research Council for Engineering Sciences.

[1]J. G. Bednorz and K. A. Müller, Z. Phys. B **64**, 189 (1986).
[2]See, for instance, P. A. P. Lindberg, Z.-X. Shen, W. E. Spicer, and I. Lindau, Surf. Sci. Rep. **11**, 1 (1990).
[3]See, for instance, W. E. Pickett, Rev. Mod. Phys. **61**, 433 (1989).
[4]J. Orenstein, G. A. Thomas, D. H. Rapkine, C. G. Bethea, B. F. Levine, B. Batlogg, R. J. Cava, D. W. Johnson, Jr., and E. A. Rietman, Phys. Rev. B **36**, 8892 (1987), and references therein.
[5]J. C. Fuggle, P. J. W. Weijs, R. Schoorl, G. A. Sawatzky, J. Fink, N. Nücker, P. J. Durham, and W. M. Temmerman, Phys. Rev. B **37**, 123 (1988).
[6]A. Fujimori, E. Takayama-Muromachi, Y. Uchida, and B. Okai, Phys. Rev. B **35**, 8814 (1987).
[7]P. Marksteiner, S. Massida, Jaejun Yu, A. J. Freeman, and J. Redinger, Phys. Rev. B **38**, 5098 (1988).
[8]J. Ghijsen, L. H. Tjeng, H. Eskes, G. A. Sawatzky, and R. L. Johnson, Phys. Rev. B **42**, 2268 (1990).
[9]T. Takahashi, F. Maeda, H. Arai, H. Katayama-Yoshida, Y. Okabe, T. Suzuki, S. Hosoya, A. Fujimori, T. Shidara, T. Koide, T. Miyahara, M. Onoda, S. Shamoto, and M. Sato, Phys. Rev. B **36**, 5686 (1987).
[10]Z.-X. Shen, J. W. Allen, J. J. Yeh, J.-S. Kang, W. Ellis, W. E. Spicer, I. Lindau, M. B. Maple, Y. D. Dalichaouch, M. S. Torikachvili, J. Z. Sun, and T. H. Geballe, Phys. Rev. B **36**, 8414 (1987).
[11]R. L. Kurtz, R. L. Stockbauer, D. Mueller, A. Shih, L. E. Toth, M. Osofsky, and S. A. Wolf, Phys. Rev. B **35**, 8818 (1987).
[12]Z.-X. Shen, P. A. P. Lindberg, P. Soukiassian, C. B. Eom, I. Lindau, W. E. Spicer, and T. H. Geballe, Phys. Rev. B **39**, 823 (1989).
[13]S. C. Wu, C. K. C. Lok, J. Sokolov, F. Jona, and A. Taleb-Ibrahimi, Phys. Rev. B **39**, 1058 (1989).
[14]G. van der Laan, B. T. Thole, H. Ogasawara, Y. Seino, and A. Kotani, Phys. Rev. B **46**, 7221 (1992).
[15]G. van der Laan, M. Surman, M. A. Hoyland, C. F. J. Flipse, B. T. Thole, Y. Seino, H. Ogasawara, and A. Kotani, Phys. Rev. B **46**, 9336 (1992).
[16]L. H. Tjeng, C. T. Chen, J. Ghijsen, P. Rudolf, and F. Sette, Phys. Rev. Lett. **67**, 501 (1991).
[17]Y. Seino, H. Ogasawara, A. Kotani, B. T. Thole, and G. van der Laan, J. Phys. Soc. Jpn. **61**, 1859 (1992).
[18]L. H. Tjeng, C. T. Chen, and S-W. Cheong, Phys. Rev. B **45**, 8205 (1992).
[19]R. Nyholm, S. Svensson, J. Nordgren, and A. Flodström, Nucl. Instr. Methods Phys. Res. Sect. A **246**, 267 (1986).
[20]J. N. Andersen, O. Björneholm, A. Sandell, R. Nyholm, J. Forsell, L. Thånell, A. Nilsson, and N. Mårtensson, Synch. Radiat. News **4**, (4), 15 (1991).
[21]M. Qvarford, N. L. Saini, J. N. Andersen, R. Nyholm, E. Lundgren, I. Lindau, J. F. van Acker, L. Leonyuk, S. Söderholm, and S. A. Flodström, Physica C **214**, 119 (1993).
[22]D. B. Mitzi, L. W. Lombardo, A. Kapitulnik, S. S. Laderman, and R. D. Jacowitz, Phys. Rev. B **41**, 6564 (1990).
[23]S. A. Sunshine, T. Siegrist, L. F. Schneemeyer, D. W. Murphy, R. J. Cava, B. Batlogg, R. B. van Dover, R. M. Fleming, S. H. Glarum, S. Nakahara, R. Farrow, J. J. Krajewski, S. M. Zahurak, J. V. Waszczak, J. H. Marshall, P. Marsh, L. W. Rupp, Jr., and W. F. Peck, Phys. Rev. B **38**, 893 (1988).

[24]J. B. Torrance, Y. Tokura, S. J. LaPlaca, T. C. Huang, R. J. Savoy, and A. I. Nazzal, Solid State Commun. **66**, 703 (1988).

[25]J. M. Tarascon, W. R. McKinnon, P. Barboux, D. M. Hwang, B. G. Bagley, L. H. Greene, G. W. Hull, Y. LePage, N. Stoffel, and M. Giroud, Phys. Rev. B **38**, 8885 (1988).

[26]C. C. Torardi, M. A. Subramanian, J. C. Calabrese, J. Gopalakrishnan, E. M. McCarron, K. J. Morrissey, T. R. Askew, R. B. Flippen, U. Chowdhry, and A. W. Sleight, Phys. Rev. B **38**, 225 (1988).

[27]J. J. Yeh and I. Lindau, At. Data Nucl. Data Tables **32**, 1 (1985).

[28]The fact that not only the satellite, but also the main valence band, are enhanced at resonance and its implication on the nature of the states near the Fermi level, has been previously discussed by Tjeng *et al.* (Ref. 16).

[29]M. Grioni, J. F. van Acker, M. T. Czyżyk, and J. C. Fuggle, Phys. Rev. B **45**, 3309 (1992).

[30]See, for instance, Z.-X. Shen, P. A. P. Lindberg, B. O. Wells, D. B. Mitzi, I. Lindau, W. E. Spicer, and A. Kapitulnik, Phys. Rev. B **38**, 11 820 (1988).

[31]G. van der Laan, C. Westra, C. Haas, and G. A. Sawatzky, Phys. Rev. B **23**, 4369 (1981).

[32]S. N. El Ibyari, W. N. Asaad, and E. J. McGuire, Phys. Rev. A **5**, 1048 (1972).

[33]E. Antonides, E. C. Janse, and G. A. Sawatzky, Phys. Rev. B **15**, 1669 (1977).

[34]E. J. McGuire, in *Atomic Inner-Shell Processes,* edited by Bernd Crasemann (Academic, New York, 1975).

[35]C. Froese Fischer, Comput. Phys. Commun. **14**, 145 (1978).

[36]R. D. Cowan, *The Theory of Atomic Structure and Spectra* (University of California Press, Berkeley, 1981).

[37]I. P. Grant, B. J. McKenzie, P. H. Norrington, D. F. Mayers, and N. C. Pyper, Comput. Phys. Commun. **21**, 207 (1980).

[38]It should be noted that the satellite line shapes on resonance obtained in this work also agree with the CuO cluster calculation by Seino *et al.* (Ref. 17).

[39]U. Fano, Phys. Rev. **124**, 1866 (1961).

[40]M. F. López, A. Höhr, C. Laubschat, M. Domke, and G. Kaindl, Europhys. Lett. **20**, 357 (1992). See also, L. H. Tjeng, *ibid.* **23**, 535 (1993); M. F. López, C. Laubschat, and G. Kaindl, *ibid.* **23**, 538 (1993).

[41]P. A. P. Lindberg, Z.-X. Shen, B. O. Wells, D. B. Mitzi, I. Lindau, W. E. Spicer, and A. Kapitulnik, Phys. Rev. B **40**, 8769 (1989).

[42]J. Zaanen, G. A. Sawatzky, and J. W. Allen, Phys. Rev. Lett. **55**, 418 (1985).

[43]It should be pointed out that because of the used calibration procedure, the values obtained for ΔE_{VB} are insensitive to any artifact in the absolute calibration. This is so because all spectra in Fig. 5 are parts of spectra covering energy regions which also include the Bi 5*d* level. The calibrated values obtained for Bi 5*d* in spectra *A* and *B* are used to calibrate spectra *C* and *D* in Fig. 5.

[44]J. Park, S. Ryu, M. Han, and S.-J. Oh, Phys. Rev. B **37**, 10 867 (1988).

[45]A more thorough analysis of the magnitudes of U_{dd} and Δ_{pd} for Bi2201 and Bi2212 will be presented elsewhere by Chiaia *et al.* The analysis is done by applying a cluster configuration-interaction model (see Ref. 10) to both Cu 2*p* XPS data and the present valence-band resonant photoemission data.

[46]M. Qvarford, J. N. Andersen, R. Nyholm, J. F. van Acker, E. Lundgren, I. Lindau, S. Söderholm, H. Bernhoff, U. O. Karlsson, and S. A. Flodström, Phys. Rev. B **46**, 14 126 (1992).